Automatic Registration of 3D MR Images with a Computerized Brain Atlas

Olivier Cuisenaire†, Jean-Philippe Thiran†, Benoît Macq†,
Christian Michel†, Anne De Volder ‡ and Ferran Marquès *

†: Université catholique de Louvain,
Laboratoire de Télécommunication et Télédétection,
Place du Levant 2, B-1348 Louvain-la-Neuve, Belgium
email: Cuisenaire@tele.ucl.ac.be

‡: Université catholique de Louvain,
Laboratoire de Tomographie par Positron, Louvain-la-Neuve, Belgium
*: Universitat Politècnica de Catalunya, Barcelona, Spain

ABSTRACT

We present an automatic and unsupervised method for non-rigid registration of 3D Magnetic Resonance (MR) Images with the Stockholm Computerized Brain Atlas (CBA). This method can be used in the context of multimodal medical image registration, fusion and automatic brain segmentation. In these applications anatomical images (MR) are coregistered with low spatial resolution functional imaging modalities (PET and SPECT) and fused with the neurological database of the CBA.

The proposed matching method is based on the minimization of a 3D Chamfer distance function between the surface of the brain extracted from the MR Image and the CBA brain surface. The surface-to-surface distance function is efficiently calculated by using a precomputed point-to-surface Euclidean distance map.

The non-rigid inter-patient transformation of the CBA is modeled by a generalized 3D second order transformation. This transformation is easily differentiable and, as a consequence, fast and efficient minimization methods can be used. First, a quasi-rigid, first order transformation is computed. Then, the matching is improved by introducing the second order coefficients into the transformation. After this global matching, a local adaptation of the CBA is performed by a morphing method.

The combination of a second order global transformation with a 3D local morphing allows to obtain a registration accuracy of one pixel, i.e. a mean distance between the surface of the brain in the MR Image and the CBA of one pixel, which is significantly better than what can be expected from a human operator.

Keywords: automatic image registration, computerized brain atlas, MR Images, 3D distance function

1 INTRODUCTION

Image interpretation in neurology often requires the use of an individual providing accurate sulci/gyri identification. This is not only true for high spatial resolution modalities such as CT or MRI, but also for medium to low spatial resolution images as metabolic (functional) maps obtained with PET or SPECT. The brain atlas may either be obtained by delineation of the most relevant sulci in individual MRI 3D datasets and their subsequent fusion into anatomic or functional data[1] and/or by using non linear transformation of a standard atlas, which is the object of the present work.

Manual or automatic delineation of the major brain sulci can be carried out on good quality MRI surfaces but does not provide labelling of the structures. Atlas-based sulcal identification is a viable alternative despite a high individual gyral variability,[2] since the proposed templates are generally not too far from their targets. The CBA database[3] is based on anatomical information obtained from cryosectionned brains and provides localization of sulci and gyri, Brodmann cytoarchitectonic areas and basal ganglia. This atlas is adjusted to individual brain images which supplies templates for sulci labelling and delineation of the Brodmann areas.

Matching the CBA with individual MRI datasets is currently done manually by chosing the optimum parameters for a number of elementary transforms which are combined into a general 3D second degree transform.[4] The optimization criterion is the visual matching of the transformed CBA objects, mainly the brain surface and the ventricular system, with the MR images. Although the efficiency of this method has been demonstrated,[5] it suffers from being both time-consuming and operator dependent.

In the automatic registration procedure we propose, the optimization of the transformation coefficients is performed through the iterative minimization of a matching criterion. The following section presents the matching criterion as a Chamfer distance[8] on simplified cortical and ventricular surfaces and a fast computation method based on a precomputed distance map. In section 3, the global transformation model and the computation of its optimal parameters are described, while section 4 presents the local transformation used as a post-processing tool. The results obtained are described in section 5 and discussed in section 6, which also compares the respective advantages of the manual and the automatic matching procedures.

2 MATCHING CRITERION

The first task when matching a MR image with the CBA is to define a suitable matching criterion, that is a criterion both relevant and easily computable. We choose the Chamfer distance between two reduced sets of points, the simplified outer surfaces of the MRI and CBA brains. We shall first explain how these surfaces are obtained, then formalize the distance function between the two sets of points, and finally present how distance maps allow to compute the distance function in an efficient way.

2.1 Simplified Surfaces

In this work, we start from MR brain images which have been previously segmented with the directional watershed algorithm,[6] as shown on figure 1a-c. This method achieves high quality brain surfaces (fig 1.d) including the ventricular system. However these surfaces are too detailed to be used in the matching procedure. First, the use of the sulcal patterns would represent a potential source of error due to the intrinsic sulcal variability. Moreover, the complexity of a criterion based on a detailed surface is much higher than the one obtained with a simplified one as described in section 3. The use of the detailed brain surface would lead to a waste of computation time and, more dramatically, would produce a non-convex criterion with respect to the transformation parameters.

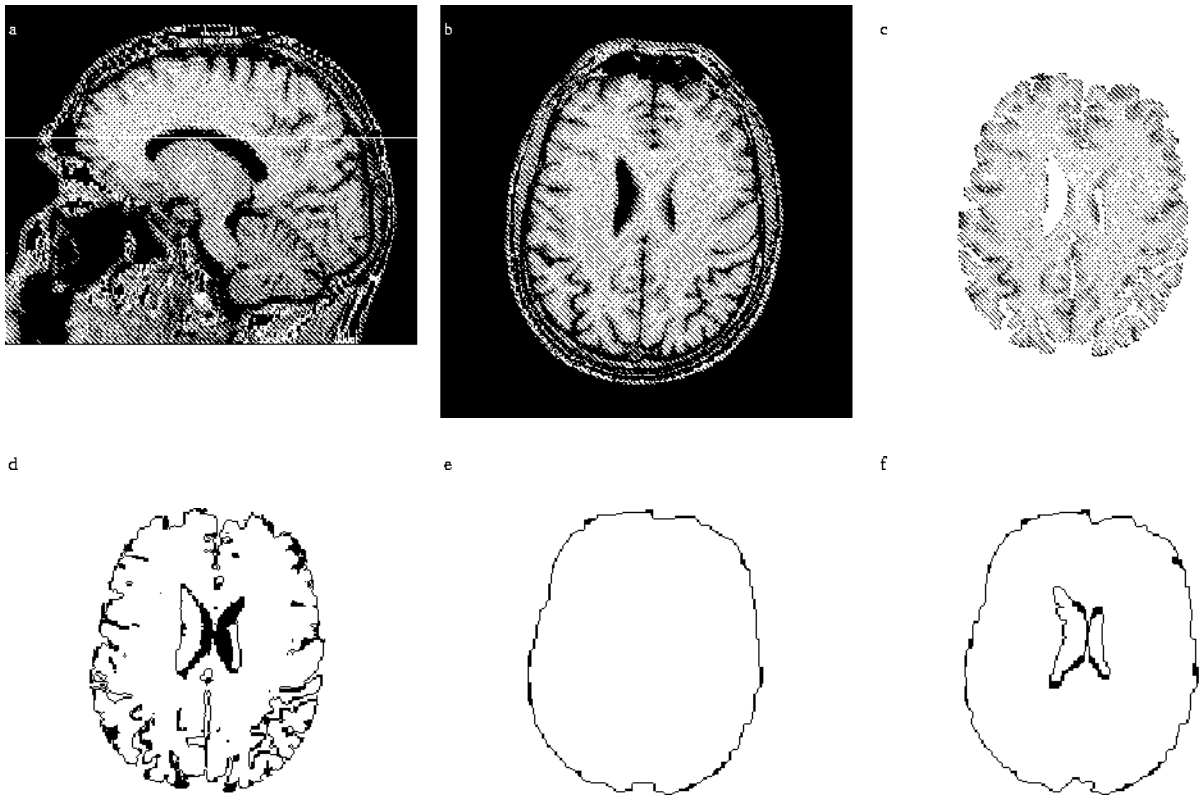

Figure 1: Extraction of the simplified cortical and ventricular surface: a & b) Original MR Image: white line on sagittal view (a) gives the level of the horizontal plane (b). c) Brain image after segmentation with directional watersheds d) Detailed brain surfaces e) Simplified cortical surface f) Simplified cortical surface and ventricular system.

This would prevent the use of efficient minimization techniques.

Therefore, we simplify the brain object by applying to it a binary morphological closing.[7] This operation has the property of filling holes of a size smaller than the structuring element. Thus, by choosing this size appropiately, one can remove the sulci and, if necessary the ventricular system from the criterion's set of point. In section 3, in order to match the complexity of the criterion with the one of the transform we search, we will use either the outer surface alone (figure 1.e) or this surface and the ventricular system (figure 1.f).

2.2 Chamfer distance

We define the Chamfer distance[8] between the sets of points S_{mob} and S_{ref} (the mobile and reference surfaces, respectively) as the quadratic mean of the distances from each point of S_{mob} to S_{ref}. The distance between one point and S_{ref} is the smallest distance between this point and any point of S_{ref}. Formally, we have

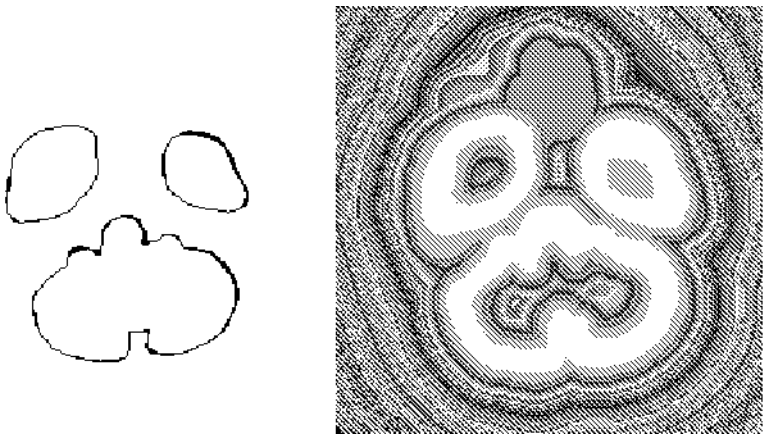

Figure 2: Distance map generation: one band of S_{ref} (left) and corresponding distance map in random colors

$$D(S_{mob}, S_{ref}) = \left(\frac{\sum_{x \in S_{mob}} d^2_{S_{ref}}(x)}{cardinal(S_{mob})} \right)^{\frac{1}{2}} \quad (1)$$

$$d_{S_{ref}}(x) = min\{d(x, y) \mid y \in S_{ref}\} \quad (2)$$

In this last formula, we use the true Euclidean point to point distance instead of an approximated 3-4-5 distance transformation as often proposed.[8,9] Indeed, this is a better choice since we want to use the gradient of the criterion. Although this represents a computational burden, this calculation is performed only once and will not affect significantly the global registration time.

2.3 Distance Map

The evaluation of the distance criterion being central in any iterative minimization method, a fast computing procedure is proposed. We produce a distance map by precomputing $d^2_{S_{ref}}(x)$ from equation 2 for all points in a discrete volume including S_{ref}. Subsequently, the evaluation of equation 1 will only require the computation of a sum.

The Euclidean 3D distance map can be efficiently generated by using a region growing algorithm based on hierarchical queues (similarly to the watershed algorithm[6]).

Since we choose S_{ref} as the CBA surface and S_{mob} for the MR outer brain surface, the computation of the distance map from S_{ref} has to be performed only once. If stored, it may subsequently be used for any registration. Figure 2 illustrates a cut through the distance map.

3 GLOBAL TRANSFORMATION MODEL

The global transformation $y = T(x)$ from the MRI S_{mob} to the CBA S_{ref} is modeled by a linear combination of N elementary scalar functions $f_j(x)$ for each coordinate $y_i (i = 0, 1, 2)$ of $\mathbf{y}$. Formally,

$$y_i = \sum_{j=0}^{N-1} \alpha_{ij} . f_j(x) \tag{3}$$

With this model, the general 3D first degree transform is represented with N=4 and $f_j(x) = 1, x_0, x_1, x_2$, and thus 12 coefficients α_{ij}. The general second degree transform uses N=10 and $f_j(x) = 1, x_0, x_1, x_2, x_0^2, x_1^2, x_2^2, x_0x_1, x_0x_2, x_1x_2$, and thus 30 coefficients α_{ij}. While this model is sufficiently general to provide the 2 transforms we are interested in, it cannot, for instance, model a rotation as a unique parameter.

The matching efficiency of a given transform $T_{\alpha_{ij}}(x)$, defined by its 3N coefficients α_{ij}, is assessed by $D(T(S_{mob}), S_{ref})$ where $T(S_{mob})$ is the set of points $y = T(x)$ for all $x \in S_{mob}$ and D(,) is the Chamfer distance defined in equation 1. In order to simplify the notations, we choose the equivalent criterion:

$$M(\alpha_{ij}) = D^2(T(S_{mob}), S_{ref}).cardinal(S_{mob}) = \sum_{x \in S_{mob}} d^2_{S_{ref}}(T_{\alpha_{ij}}(x)) \tag{4}$$

Finding the optimal transform $T_{\alpha_{ij}}(x)$ is thus equivalent to minimizing the criterion $M(\alpha_{ij})$ in the coefficient space. This is possible, despite the high number of coefficients, thanks to the two following points:

- First, thanks to the appropriate choice of the surfaces S_{mob} and S_{ref} in section 2.1, the criterion $M(\alpha_{ij})$ is convex in the space of coefficients α_{ij}, at least in a reasonable range (for instance rotations of less than 30 degrees around the matching point).
- Second, the gradient of $M(\alpha_{ij})$ in the space of α_{ij} can be easily computed as the partial derivatives are written

$$\frac{\delta M(\alpha_{ij})}{\delta \alpha_{ij}} = \sum_{x \in S_{mob}} \frac{\delta(d^2_{S_{ref}}(y))}{\delta y_i} . \frac{\delta y_i}{\delta \alpha_{ij}} \tag{5}$$

  with $y = T_{\alpha_{ij}}(x)$. In this formula, the first term of the product can be numerically approximated from the distance map of $d^2_{S_{ref}}(x)$ and the second term comes straight from equation 3. Thus, the partial derivatives of $M(\alpha_{ij})$ are evaluated as

$$\frac{\delta M(\alpha_{ij})}{\delta \alpha_{ij}} = \sum_{x \in S_{mob}} \frac{d^2_{S_{ref}}(y + e_i) - d^2_{S_{ref}}(y - e_i)}{2.pixelsize} . f_j(x) \tag{6}$$

  with e_i the unit vector for coordinate i. A straightforward computation of this formula is possible since $d^2_{S_{ref}}(x)$ are available from the distance map.

Therefore, we can use a gradient based method to efficiently minimize $M(\alpha_{ij})$. In practice, we use an iterative algorithm modifying all coefficients proportionally to their partial derivative. Such modifications are normalized so that the change vector in the α_{ij} space as a constant norm. This constant is lowered each time the main highest partial derivative $\frac{\delta M(\alpha_{ij})}{\delta \alpha_{ij}}$ does change of sign.

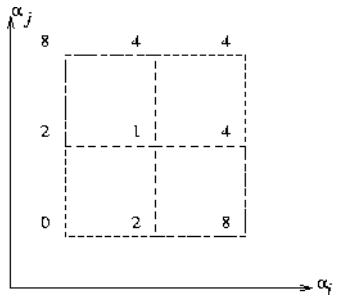

Figure 3: A local minimum appears in the central point (value 1) due to the discrete nature of the α_i, α_j space, although the continuous function used to generate this example ($z = 2x^2 + 2y^2 - 3xy$) is convex.

Furthermore, the efficiency of the minimization is improved by first orthogonalizing and normalizing the base functions $f_j(x)$ relatively to the S_{mob} set.

Finally, the choice of a gradient based algorithm is not only motivated by speed considerations. It is also an efficient way of avoiding local minima due to the discrete nature of the distance map. Indeed, as shown in figure 3, a convex continuous function does not always remain convex after being discretized. This could lead to mismatching if stuck in a local minimum.

On this example, we can see that an algorithm that would optimize the parameters one by one would fall into the local minimum, while a gradient based method can successfully avoid this bias.

4 LOCAL TRANSFORMATION

Due to the high variability in brain shape and size, the global transform described in the previous section will only provide an approximate registration. Improving this result by increasing the order of the global transform seems unrealistic. First, the possible improvement is negligible compared to the additional computational cost. Second, there is no obvious CBA structure that can be added to S_{ref} to match the complexity of the criterion to that of a third degree transform. Furthermore, this introduces a risk of instability in the minimization.

Therefore, a local transform is the best choice for further improving the accuracy of the registration. We propose a morphing transform which is described in the four following steps:

- The S_{mob} space is divided into a regular mesh of cubes (figure 4.a). In practice, we use 8x8x8 cubes.
- For each cube in which a significant number of points from S_{mob} are located, the best local translation is computed (figure 4.b). This is done by applying the algorithm of section 3 with N=1 and $f_0 = 1$.
- The local result are extended to the remaining cubes (those not containing a significant number of points of S_{mob}) by assigning a compatible translation to them (figure 4.c).
- The transform is made continuous by assuming the translations are only valid for the central point of the cubes and by interpolating the translation vectors for points between the cube centers.

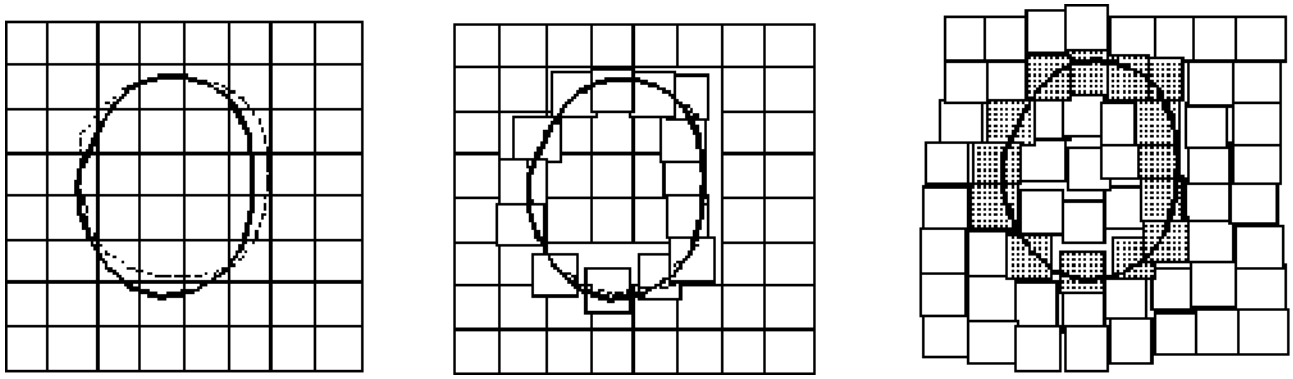

Figure 4: Steps of the local transform algorithm.

5 RESULTS

The natural way for dividing the transform from the MR image to the CBA is to consider the combination of two transforms: a rigid transform (translation, rotation and if necessary scaling) corresponding to the variable location of the head in the imaging device, and a more complex deformation (second degree transform) which takes care of the inter-patient brain variability. This division is currently used in the manual registration.

The transform described in equation 3 of section 3 cannot model a rigid transform since it requires linking the coefficients α_{ij}. Therefore, the automatic registration divides the transform into a first and a second degree transform. Mathematically, the first degree transform is necessary to bring $T(S_{mob})$ into the convexity domain of the criterion for the second degree transform. The effects of the first degree, second degree and local transforms are shown in figure 5.

The transforms are computed from the MRI to the CBA. This spares the generation of a distance map from S_{ref} through the use of a stored map. On the other hand, the CBA to MRI transforms are usually more interesting since they are needed to display CBA structures on the MRI. The invert transforms are easily computed, analytically for the first degree transform and numerically for the second degree and local transforms.

The first degree transform reduces the Chamfer distance between S_{ref} and $T(S_{mob})$ from 13.4 to 3.4 (the unit is the size of the horizontal pixel, the image of our example has anisotropic voxels with the axial pixel size 2.33 times bigger than the horizontal or tomographic one).

As mentioned in section 3, the second degree transform requires the inclusion of the ventricular system into S_{ref}. The lack of information in the center of the image, when ventricles are not considered, does not allow to achieve a unique minimum since the x_i^2 base functions model a relative translation of the center and the edges of the image. In our example, the Chamfer distance is reduced from 3.4 to 3.1. This illustrates the small improvement obtained when increasing the order of the global transform and it justifies the use of a local alternative.

For the local transform, we use a simplified S_{ref} without ventricles. This is obviously not optimal since a local transform could take further details such as sulci into account. Unfortunately, more complex criteria often lack robustness. Nevertheless, this not optimal criterion still has the property of improving the local registration accuracy near the edge of the image while its center is only slightly affected. The Chamfer distance is reduced from 3.1 to 2.36. This value is roughly the size of the vertical (axial) pixel in our example.

This result might be improved for further applications of the local transform by using a mesh of smaller and smaller cubes. Nonetheless, this is irrelevant as long as the criterion S_{ref} does not include more details.

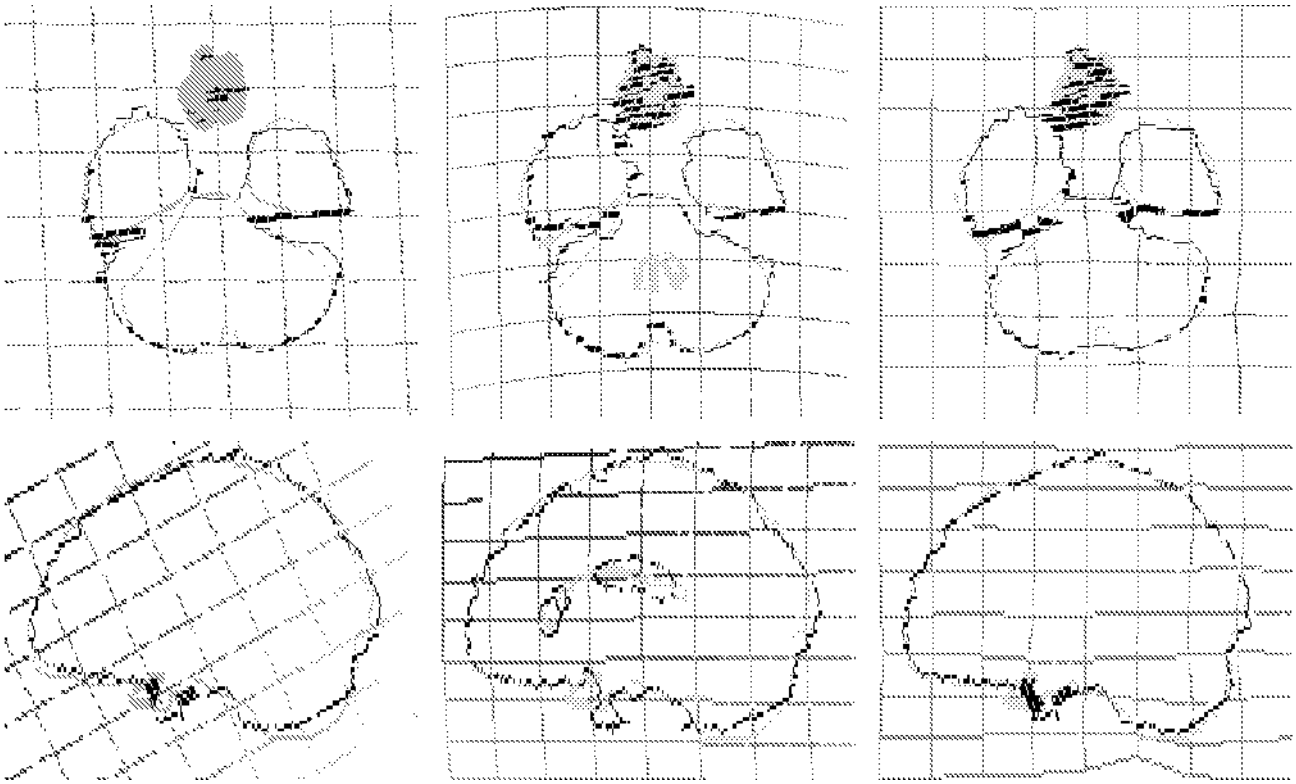

Figure 5: First degree, second degree and local transforms of the brain surface (left to right). The CBA surface S_{ref} and the MRI transformed surface $T(S_{mob})$ are displayed in grey and black, respectively. They are overlayed with a cubic grid which follows the same transformations.

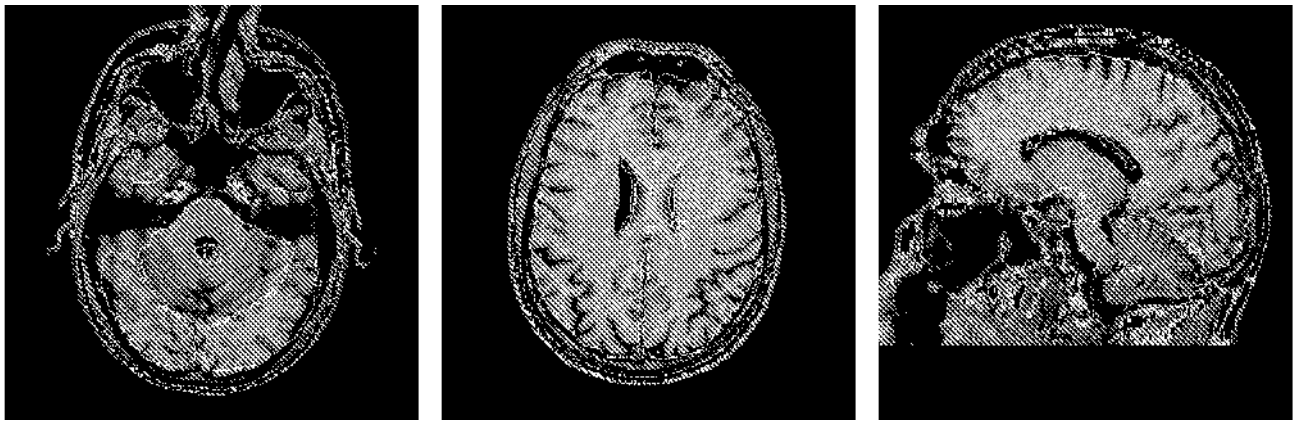

Figure 6: Projection of the CBA "detailed surface" and "ventricular system" regions into the MRI dataset. Two horizontal and a sagittal planes are shown.

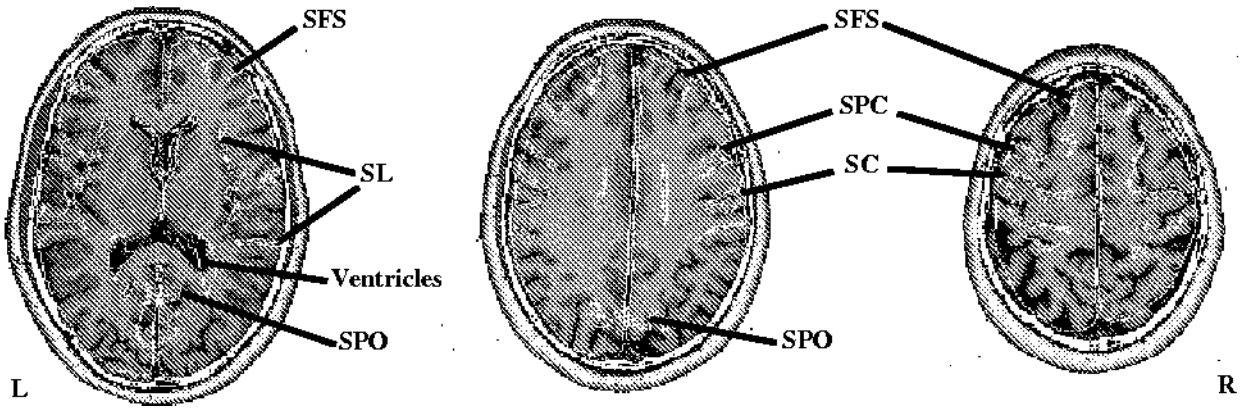

Figure 7: Individual MR images of the brain at the level of the basal ganglia (a) and 2 and 4 cm above that plane. Transformed atlas structures are superimposed.

The final result is shown in figure 6 as the projection of the two main CBA structures into the MR image.

6 DISCUSSION

The automatic procedure has several advantages when compared with the current manual one[4]:

- It is quicker and does not require as much expertise or training.
- It takes all slices simultaneously into account, while the CBA graphic user interface does not allow to display all of them.
- A human operator performs what can merely be described as a parameter by parameter minimization, which can lead to a local minimum, as illustrated in figure 3 of section 3.
- The local transform (morphing) cannot be performed by a human operator.

Anyhow, several interesting features provided by the manual registration program are not implemented in our procedure:

- An operator may favor the accurate registration of a definite region of the brain, relaxing the overall matching constraint.
- Additional information may be used in the matching criteria. For instance, the location of the central, pre and post-central sulci is often used to check the accuracy of a chosen transform.

The ultimate aim of computerized atlases is to achieve a 3D representation of all identifiable anatomical structures in the individual brain. As shown in figure 7, this objective is well reached by the present work which allows to delineate unambiguously the sylvian fissure (sl), the superior frontal (ssf), the precentral (spc), the central (sc) and the parieto-occipital (spo) sulci. As clearly seen on the top slice, the template for the left

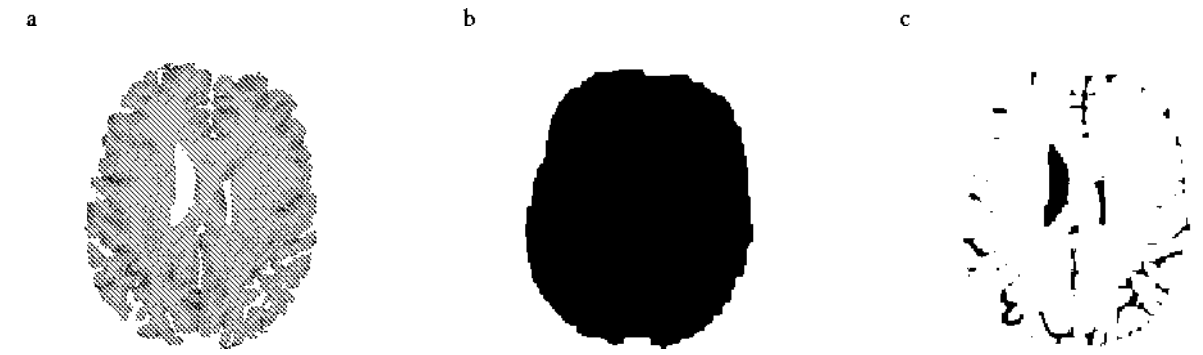

Figure 8: Extraction of the sulci from the segmented MRI: a) segmented brain from MRI b) morphological closing of a. c) morphological top-hat of a.

superior frontal sulcus does not match with the one of the subject despite the perfect matching of that sulcus on the contralateral hemisphere. Inter-hemispheric variations in the topography of the sulcal patterns represents an intrinsic limitation in this approach.

The use of the detailed brain surface allows to extract 3D sulcal shapes using a morphological top-hat (difference between the morphological closing of an object and the original object), as illustrated in figure 8. Unfortunately, this does not provide labeling of the structures. A further perspective of this work would deal with the automatic labeling of the sulci based on a proximity criterion.

7 CONCLUSION

Our automatic registration method provides satisfactory results by using the reduced information from the brain surface and the ventricular system.

On the other hand, this reduced information can be computed from a low resolution functional image, thus suggesting the possibility of a direct matching between the CBA and a PET image, without the need of a MRI. In that case, the basal ganglia (caudate, putamen and thalamus) could substitute the ventricles.

Finally, this method could be applied to the registration of multi-modal images obtained in a single patient. For this purpose, the transformation model is simplified as a single first degree transform modeling the rigid transform and scaling between the two modalities.

8 ACKNOLEDGEMENTS

Special thanks to Lennart Thurfjell, C. Bohm, Lars Eriksson and Martin Ingvar, from Karolinska for providing us with the CBA computerized brain database.

O.C. and J-P.T are funded by the Belgian FRIA (Fonds pour la Formation à la Recherche dans l'Industrie et l'Agriculture), B.M. and C.M. are senior research associates of the Belgian National Fund for Scientific Research.

9 REFERENCES

[1] C. Michel, M. Sibomana, A. Coppens, A. Bol, A. De Volder, C. Grandin, V. Warscotte, J-P. Thiran and B. Macq. Interactive Delineation of Brain Sulci and their merging into Functional PET images. submitted to *IEEE-Trans. Nucl. Sci.*, 1995

[2] P.E. Roland and K. Zilles. Brain atlases a new research tool. *Trends in Neurosciences* vol. 17 pp. 458-67, 1994.

[3] C. Bohm, T. Greitz, D. Kingsley, B.M. Berggren and L. Olsson. Adjustable computerized stereotaxic brain atlas for transmission and emission tomography. *Am J. Neuroradiology* vol. 4 pp. 731–733, 1983.

[4] L. Thurfjell, C. Bohm, T. Graitz and L. Eriksson. Transformations and Algorithms in a Computerized Brain Atlas. *IEEE Trans. on Nuclear Sciences*, vol. 40 pp. 1187–1191, 1993

[5] R.J. Seitz, C. Bohm, T. Greitz, P.E. Roland, L. Eriksson, G. Blomqvist, G. Rosenqvist and B. Nordell. Accuracy and Precision of the Computerized Brain Atlas Program for Localization and Quantification in Positron Emission Tomography *Journal of Cerebral Blood Flow and Metabolism*, vol. 10 pp. 443–457, 1990

[6] V. Warscotte, J.-P. Thiran, B. Macq, C. Michel and P. Fourez. Accurate Segmentation of 3D Magnetic Resonance Images of the Head using a Directional Watershed Transform. Montreal, September 1995, IEEE Engineers in Medicine and Biology Conference.

[7] M. Sonka, V. Hlavac and R. Boyle. *Image Processing, Analysis and Machine Vision.* Chapman & Hall, 1993, Chap 10: Mathematical Morphology, pp. 422–442.

[8] G. Borgerfors. Hierarchical Chamfer Matching: A parametric edge matching algorithm. *IEEE transactions on Pattern Analysis and Machine Intelligence* vol. 10 pp. 849–865, 1988.

[9] J.F. Mangin, V. Froin, I. Bloch, B. Bendriem and J. Lopez-Krahe. Fast Non-supervised 3D registration of PET and MR Images from the Brain *Journal of Cerebral Blood Flow and Metabolism* vol. 14 pp. 749–792, 1994.